Optical Response of Ultrafine Spherical Silver Nanoparticles Arranged in Hexagonal Planar Arrays Studied by the DDA Method†

Hervé Portalès,[#,§] Nicola Pinna,[‡] and Marie-Paule Pileni*[,#,§]

Université Pierre et Marie Curie Paris 6, UMR 7070, LM2N, 4 place Jussieu, 75005 Paris, France, Centre National de la Recherche Scientifique, UMR 7070, LM2N, 4 place Jussieu, 75005 Paris, France, and Department of Chemistry, CICECO, University of Aveiro, 3810-193 Aveiro, Portugal

Received: November 28, 2008

Absorption spectra of nanosized spherical silver particles hexagonally arranged in planar arrays have been calculated using the discrete dipole approximation (DDA). The silver dielectric function used in the calculations is size-corrected in order to account for the ultrafine particle size of 5 nm in diameter. The optical anisotropy arising from the dimensionality of the planar array of close-packed nanoparticles is clearly revealed in the absorption spectra by the splitting of the surface plasmon resonance (SPR) in two bands corresponding to the longitudinal and transverse modes. Under p-polarized light, the amplitude of the splitting is observed to sensitively increase for decreasing interparticle spacing. This behavior makes it possible to well distinguish the two SPR bands under the requirement that the interparticle spacing should be smaller than around one particle radius. Indeed, for larger interparticle spacing, the two plasmon modes tend to superimpose, so that the profile of the resulting single band looks nearly the same as the one of an isolated nanoparticle.

I. Introduction

A characteristic feature in the optical spectra of metal nanoparticles is the dipolar surface plasmon resonance[1] (SPR) band. This latter can be attributed to the collective oscillation of the conduction electrons of the nanoparticle due to their resonant coupling with the electric field of the incident light. Experimentally, the frequency and strength of these oscillations strongly depend on the size[2,3] and shape[4−7] of the nanostructures, their composition,[8,9] and also the local dielectric environment. In addition to these experimental investigations, various numerical approaches have been developed to study the optical properties of metal nanoparticles, with the aim to better understand the influence of the particle size, shape, and environment on the SPR characteristics.[10−12] Controlling some of these parameters allows manipulation of the optical properties of the nanostructure[7] and, in particular, control over how it scatters and absorbs light[13,14] and how the local electric field is modified.[15] Therefore, such a control plays a crucial role in the development of promising technological applications based on SPR[16−18] and still drives great interest in the field of nanomaterials research.[19]

Most of the numerical methods were first devoted to simulate the optical response of isolated spherical particles in various environments.[13,20,21] Over the past few years, different numerical methods based on finite elements have been developed in order to study the optical response of particles with arbitrary shape and multicomposition.[22,23] Among these methods, the discrete dipole approximation (DDA) has been extensively used to simulate the extinction spectra (extinction = absorption + scattering) of metal nanoparticles with various sizes, shapes, or dielectric environments.[10−12,24−26] This method is also very useful for describing the electrodynamics of nanoparticle arrays and aggregates that have complex structures.[24] The interaction between particles in such systems can result in a drastic modification of their optical response, depending on the geometrical characteristics of the system. For instance, the Schatz group discovered few years ago that remarkably narrow plasmon line shapes[27] are produced by one- and two-dimensional arrays of silver nanoparticles with, however, the condition for making such a behavior achievable that the particle radius should be larger than about 30 nm.

In contrast, the nanoparticles that are under investigation here have diameters limited to only a few nanometers. For particles with a diameter smaller than around 10 nm, it is important to note that physical phenomena related to radiation effects (e.g., scattering process) are very weak; hence, the optical extinction can be assumed to only originate from absorption.[25] The optical properties of such ultrafine silver nanoparticles arranged in a two-dimensional (2D) compact hexagonal network have already been studied experimentally and compared with predictions deduced from different computational approaches.[28−30] From these previous studies, the optical anisotropy arising from the dimensionality of the system was clearly demonstrated through the appearance of an additional resonance at a higher energy than that of the SPR of isolated nanocrystals.

Here, we report on the use of the DDA method to point out the specific influence of the interparticle spacing on the absorption spectrum. Actually, the simulations presented aim to model close-packed self assemblies of coated spherical silver nanocrystals comparable to those that are synthesized by the chemical route in our laboratory.[31] This study essentially provides new insights on the possibility of tuning the optical properties of planar arrays of ultrafine silver nanoparticles via the control of the interparticle spacing.

The paper is organized as follows. In section II, we first describe, in detail, the DDA target built in order to mimic 2D hexagonal arrangements of silver nanoparticles. Then, we focus on the size correction of the silver dielectric function used in

† Part of the "George C. Schatz Festschrift".

* To whom correspondence should be addressed. E-mail: pileni@sri.jussieu.fr. Phone: +00 33 1 44 27 25 16.

[#] Université Pierre et Marie Curie Paris.

[§] Centre National de la Recherche Scientifique.

[‡] University of Aveiro.

10.1021/jp810478r CCC: $40.75
Published on Web 03/11/2009

our DDA simulations. In section III, we present and discuss the calculated absorption spectra.

II. The Discrete Dipole Approximation

To simulate the absorption spectra of 2D arrangements of nanometer-sized metal particles, an implementation of electrodynamic theory known as the discrete dipole approximation is used. The DDA theory was developed by Purcell and Pennypacker for astrophysical purpose to model the interaction of light with dust particles in space.[32] The original theory has then profited by some improvements[33,34] that allow use of the DDA approach to calculate the absorption, scattering, and extinction cross sections of arbitrary targets composed of individual or multiple objects of any size and shape. Furthermore, this method enables modeling of the systems composed of several materials.

The theoretical basis for the DDA has been described in more detail elsewhere[35] and is out of the scope of this paper. In a few words, the approximation involved in the DDA lies in the replacement of the continuum target by a finite array of polarizable points located in a periodic (cubic) lattice whose spatial extension is designed in such a way to mimic the geometry of the system under study. Each point acquires a dipole moment in response to both the incident plane wave field and the electric field due to the interaction with all of the other dipoles in the array. The dipole polarizations are then solved self-consistently. To perform such a calculation, the freely available program DDSCAT version 6.1 written by Draine and Flatau[36] was used. In the following sections, the geometry of the different targets involved in the DDA calculations is described as well as the procedure to account for the size dependence of the dielectric function of the silver nanoparticles.

A. Geometry of the Target. In this study, the close-packed monolayer of 5 nm silver nanoparticles is represented by a multisphere target consisting of the union of N equal-sized (diameter $2R$) and equally spaced spheres structured in a planar hexagonal array. The interparticle spacing, d, is the border-to-border distance between nearest-neighbor particles as shown in Figure 1a. In the following, the distance d will be given in terms of its ratio to the sphere diameter, that is, $d/(2R)$. Schemes of the different DDA targets investigated here are depicted in Figure 1.

As mentioned above, the DDA target is represented by an array of dipoles located on a cubic lattice. Furthermore, the meshing of the target is completely flexible and only requires the interdipole spacing to be small enough compared to the wavelength of the incident light and any structural feature of the target. This allows one to satisfactorily mimic the target and to diminish the inaccuracy arising from granularity on the surface of the target. However, both the computer memory requirement and the computing time to run the DDSCAT program increase with the total number of dipoles involved in the DDA calculations, so that it is necessary to limit the volume of the target. For these reasons, the number of particles in the target was restricted to values such as 91, 109, and 115 particles when designing arrays in hexagonal, circular, and square shapes, respectively (Figure 1a,b). Despite such a limitation, this restricted planar array is expected to fairly well mimic the optical response of a 2D system made of self-organized silver nanoparticles. Moreover, each particle was represented with around 2000 dipoles by designing the target with an interdipole spacing as small as few tenths of a nanometer. Such a fine meshing of the target was checked to achieve both a quite good shape definition and a proper convergence of the calculations. Therefore, we chose to keep it the same whatever the interparticle spacing or the number of particles.

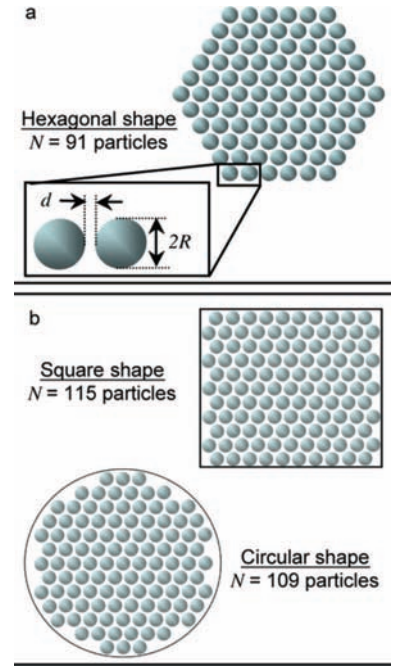

Figure 1. Schematic representation of the DDA targets used in this work. (a) Two-dimensional hexagonal array composed of $N = 91$ silver spheres (diameter $2R$) arranged in hexagonal shape with a nearest-neighbor distance, d. (b) Other shapes of 2D structures used to study the dependence of the optical response of these structures on their shape, hexagonal arrays of silver spheres arranged in square ($N = 115$ spheres) and circular ($N = 109$ spheres) shapes. All of the targets are built with a surrounding medium of refractive index $n_{ext} = 1.46$.

B. Dielectric Function. The dielectric properties of the constituting materials of the target need to be defined. The DDA requires a prescription for the determination of the dipole polarizabilities used to represent the target in order to mimic a continuum medium of dielectric function $\varepsilon(\omega)$. For this purpose, the program DDSCAT assigns to each dipole a polarizability that is related, at a given wavelength, to the specified dielectric function of the medium through the lattice dispersion relation (LDR) derived by Draine and Goodman.[37] The polarizability α_i of the ith dipole of the target can then be expressed as

$$\alpha_i = \frac{\alpha_i^{LDR}}{1 - (2/3)i(\alpha_i^{LDR}/l^3)(kl^3)} \quad (1)$$

Here, α_i^{LDR} is given by the following LDR prescription obtained, in the long-wavelength approximation ($kl \ll 1$), for an electromagnetic plane wave propagating, with a wave vector $\mathbf{k}$, on an infinite cubic lattice of interdipole spacing l

$$\alpha_i^{LDR} = \frac{\alpha_i^{CM}}{1 + (\alpha_i^{CM}/l^3)[b_1 + b_2\varepsilon_i + b_3 S\varepsilon_i](kl)^2} \quad (2)$$

where b_1, b_2, b_3, and S are the coefficients determined by integrals to include a radiative reaction correction[37] to the dipole polarizability, ε_i is the dielectric function at the lattice site i, and α_i^{CM} is the "Clausius−Mosotti" polarizability, which is given by the relation[38]

$$\alpha_i^{CM} = \frac{3l^3}{4\pi}\left(\frac{\varepsilon_i - 1}{\varepsilon_i + 2}\right) \quad (3)$$

In the general case of real bulk metals, the dielectric function $\varepsilon_{Drude}(\omega)$ consists of two additional contributions accounting for the interband and intraband electron transitions that respectively involve the bound electrons and the free electrons. The contribution of these latter to the total complex dielectric function of the bulk metal can be described by using the Drude free electron model

$$\varepsilon_{Drude}(\omega) = 1 - \frac{\omega_p^2}{\omega^2 + i\omega\gamma_0} \quad (4)$$

where ω_p is the plasma angular frequency and γ_0 a damping constant due to the scattering of the electrons with phonons, electrons, lattice defects, or impurities.

If we now consider no more bulk metals but metal nanoparticles whose size does not exceed few nanometers, as those under investigation in this study, then finite size effects influence the dielectric function and have to be taken into account. In particular, for such nanometer-sized metal particles, the conduction electrons suffer an additional damping process due to their scattering from the particle surface resulting, in a standard classical approach, in a reduced effective mean free path, L_{eff}. Therefore, one can assume the corresponding increase of the damping constant γ to be such that

$$\gamma(L_{eff}) = \gamma_0 + Av_F/L_{eff} \quad (5)$$

where A is a dimensionless parameter, usually considered to be close to unity, and v_F is the Fermi velocity. The surface dispersion effect leads to a correction of the dielectric function of the bulk metal according to the following equation[39]

$$\varepsilon(\omega, L_{eff}) = \varepsilon_{bulk}(\omega) - \varepsilon_{Drude}(\omega) + \left\{1 - \frac{\omega_p^2}{\omega^2 + i\omega(\gamma_0 + Av_F/L_{eff})}\right\} \quad (6)$$

In a geometrical probability approach,[40] L_{eff} has been shown to be size- and shape-dependent, so that the dielectric function of nanometer-sized metal particles is also expected from eq 6 to exhibit a dependence on the particle size and shape. For the present calculations, it was therefore necessary to apply such a size correction to the experimental values of the bulk silver dielectric function $\varepsilon_{bulk}(\omega)$. Note that the bulk silver wavelength-dependent dielectric function was taken from Palik's handbook.[41] To calculate now the size-corrected dielectric function of silver nanoparticles from eq 6, the following parameters[42] were used: $v_F = 1.39 \times 10^6$ m/s, $\hbar\omega_p = 8.98$ eV, and $\gamma_0 = 0.018$ eV. Furthermore, as it was established in a geometrical probability approach,[40] we assumed the effective electron mean free path for a sphere to be simply given by $L_{eff} = 4R/3$, where R is the sphere radius.

The size-corrected dielectric functions calculated for spherical silver nanoparticles of 5 and 10 nm in diameter are compared with the bulk one in Figure 2. While the real part of the complex dielectric function, $\varepsilon_1(\omega)$, appears to be weakly size-dependent, the imaginary part, $\varepsilon_2(\omega)$, sensitively increases for decreasing size in the energy range below 4 eV. Due to the ultrafine size of the silver particles that are studied here and also to the fact that they exhibit a dipolar SPR in the same energy range, the surface dispersion effect can therefore be expected to induce a significant broadening[40] of their SPR bands. Consequently, the size-corrected silver dielectric function of the particles, as deduced from eq 6, was systematically used for all of the simulations presented in this work.

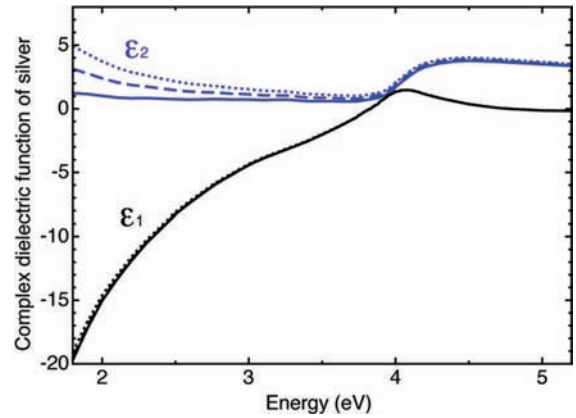

Figure 2. Real (ε_1) and imaginary (ε_2) components of the complex dielectric function of silver nanoparticles of 5 (dotted lines) and 10 nm (dashed lines) in diameter compared with those of bulk silver (solid line) from ref 41. The size-corrected dielectric functions of silver nanoparticles are calculated by using eq 6.

III. Results and Discussion

Here, we show the influence of the 2D dimensionality of close-packed nanoparticles arrays on their optical response. In particular, we propose to analyze how changing the interparticle distance influences the optical anisotropy of the nanoparticles arrangement.

The absorption spectra of $N = 91$ silver nanoparticles hexagonally arranged in a planar array were calculated using the DDA method for various angles of incidence α, ranging from 0 to 60° with respect to the normal of the 2D system (Figure 3a). It is important to mention that the incident radiation is considered to propagate along the x-axis and to be linearly polarized in a direction parallel to the y-axis. At normal incidence ($\alpha = 0°$), the planar arrangement of particles is oriented parallel to the (y,z) plane. By rotating the target around the z-axis, the illumination of the nanoparticles under different angles of incidence can be simulated. Besides, it should be noted that the external nanoparticle environment consisted of a nonabsorbing host medium of refractive index $n_{ext} = 1.46$. This value was chosen because it corresponds to the refractive index of dodecanethiol and was actually used in the simulations in order to mimic the coating of the nanoparticles, in reference to the real case of nanoparticles synthesized by soft chemical routes.[31] By doing so, the dodecanethiol molecules are assumed to form a continuous layer around each nanoparticle, which can therefore be modeled as the surrounding medium of all of the nanoparticles in the array.

The spectra obtained at various incidence angles and for five different values of the ratio $d/(2R)$ of the interparticle spacing to the sphere diameter are shown in Figure 3b−f. For very close-packed arrangements with $d/(2R) \leq 0.5$, we observe the profile of the plasmon band to be dramatically dependent on the angle of incidence. At normal incidence, the absorption spectrum only exhibits one single band. This band is due to the resonant excitation of longitudinal surface plasmon eigenmodes of the nanoparticle array by the incident radiation whose electric field

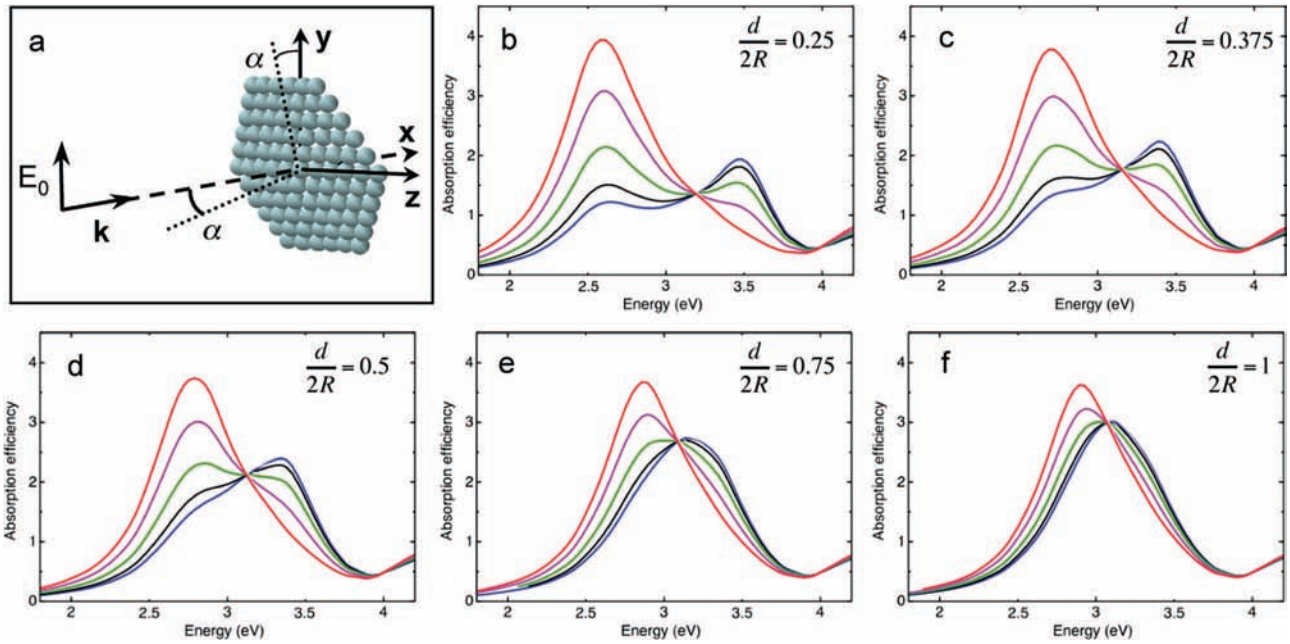

Figure 3. Dependence of calculated absorption spectra of a 2D array of $N = 91$ silver spheres ($2R = 5$ nm) on the incidence angle for different values of the relative interparticle spacing, $d/(2R)$. (a) Scheme depicting the geometry of the modeled system (light polarization + target) and defining the incidence angle, α. In the DDA target, the surrounding spheres' environment consists of a medium of refractive index $n_{ext} = 1.46$. Using such a target, absorption spectra have been calculated at various incidence angles (0 (red), 30 (violet), 45 (green), 55 (black), and 60° (blue)) in the following cases: (b) $d/(2R) = 0.25$; (c) $d/(2R) = 0.375$; (d) $d/(2R) = 0.5$; (e) $d/(2R) = 0.75$; and (f) $d/(2R) = 1$.

is parallel to the nanoparticle array. With the increase of the angle of incidence, the intensity of this band progressively decreases while a second band grows up at higher energy. To interpret the appearance of the higher energy band, one has to consider that for $\alpha \neq 0°$, the electric field of the incident radiation projects on both the parallel and perpendicular directions to the nanoparticle film, with a component along the normal direction that grows for increasing α. In such a configuration, the interaction of the incident radiation with the nanoparticles through the resonant excitation of both the longitudinal and transverse surface plasmon eigenmodes of the nanoparticle film results in the observation of two bands in the absorption spectrum. This last feature points out the optical anisotropy of the planar array of nanoparticles. It is straightforward to note here that the amplitudes of these two bands evolve in the opposite way when varying the angle of incidence.

Figure 3b−f also provides interesting information on how the optical absorption of the system evolves when the interparticle distance is varied inside of the nanoparticle arrangement. In order to simulate a nanoparticle array of comparable density, the relative interparticle spacing, $d/(2R)$, was fixed to the following values: 0.25, 0.375, 0.5, 0.75, and 1. For nanoparticles with a diameter of 5 nm, as in the present case, the corresponding distance, d, ranges then from 1.25 nm, for the more densely packed system, to 5 nm for the one with the lowest density. Since the optical spectrum of a metal particle array is influenced by the interaction between neighboring particles,[27,43−46] one can therefore expect the calculated absorption spectra to be sensitively dependent on the variation of the relative interparticle spacing. Such dependence is clearly illustrated for increasing $d/(2R)$ by a blue shift of the lower energy plasmon band, which is simultaneously observed with a red shift of the higher energy band. As a matter of fact, the increase of the interparticle spacing results in the decrease of the band splitting, in such a way that the two surface plasmon bands partially superimpose and cannot be resolved for $d/(2R) \geq 0.75$ (Figure 3e,f). To better visualize how the absorption spectrum evolves when changing the

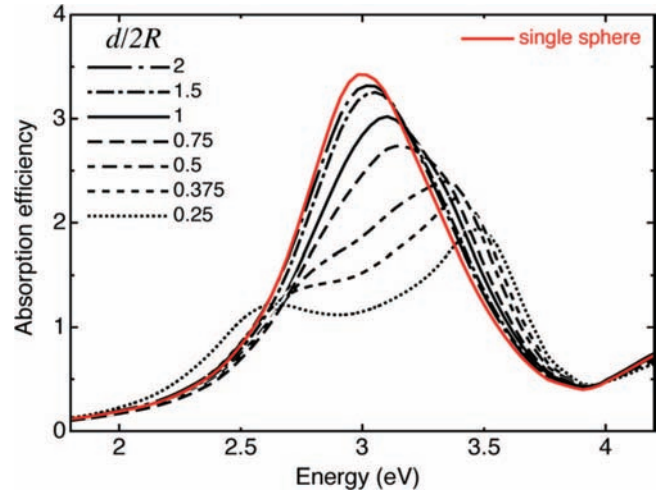

Figure 4. Dependence on the interparticle spacing (expressed as the ratio $d/(2R)$) of the calculated absorption spectra of a hexagonal array of $N = 91$ silver spheres of diameter $2R = 5$ nm for an incidence angle of $\alpha = 60°$. For comparison, these spectra are plotted together with the spectrum calculated for one single silver particle with the same size as the previous particles, which was represented by 1791 dipoles. In each case, the refractive index of the external spheres' environment is fixed at $n_{ext} = 1.46$.

interparticle spacing at a given angle of incidence, the spectra calculated for different values of $d/(2R)$ and for $\alpha = 60°$ are plotted all together in Figure 4. For the more densely packed array with $d/(2R) = 0.25$, the spectrum exhibits two distinct absorption bands, centered at 2.6 and 3.5 eV, corresponding to the longitudinal and transversal plasmon eigenmodes, respectively. The amplitude of the splitting of the SPR absorption band rapidly decreases with the increase of the interparticle spacing. The splitting is observed for compact arrangements with $d/(2R) \leq 0.5$, that is, for interparticle spacings not exceeding one particle radius. Indeed, the spectrum of the system with $d/(2R) = 1$ shows one single band centered at 3.1 eV. A further increase

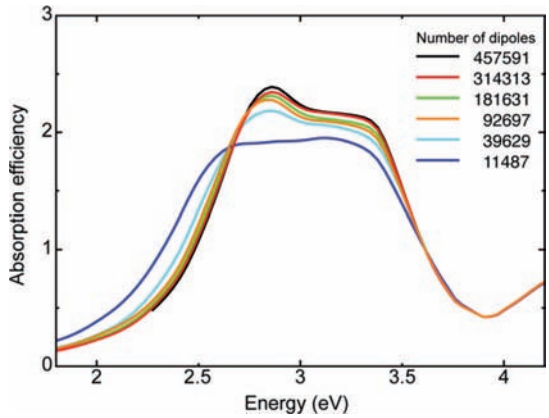

Figure 5. Absorption spectra of a hexagonal array of $N = 91$ silver spheres calculated for an angle of incidence of $\alpha = 45°$ and by using various numbers of dipoles to generate the target ($n_{ext} = 1.46$).

of the relative interparticle spacing to values as large as 1.5 or 2 (Figure 4) indicates that the surface plasmon band profile is very similar to that calculated for one isolated particle. The unique difference lies in the slight blue shift of the SPR of the densely packed particle array with respect to that of the single particle, which is peaked at 3 eV. The similitude in the SPR band characteristics (energy and bandwidth) observed between these two spectra likely reveals the weakness of the mutual interactions between neighboring particles for interparticle spacing equivalent to or greater than their own diameter ($d \geq 2R$).

All of the spectra reported in this work were calculated by using around 2000 dipoles per sphere, that is, roughly 182 000 dipoles for the full target which consists of the planar hexagonal assembly of $N = 91$ spheres. Hence, to support the reliability of these results, it is important to test the convergence of the calculations as well as the pertinence of the choice of the target shape to be used in order to properly mimic the optical response of the studied 2D system. As shown in Figure 5, the profile of the SPR spectrum remains nearly the same when increasing the number of dipoles in the target from around 92 000 to 450 000 entities. This statement argues in favor of the accuracy of the results obtained by using an average number of 182 000 dipoles. Note that to achieve the full convergence in the calculations, the use of several hundred thousand dipoles is required in the DDA target. However, it should also be noticed from the spectra plotted in Figure 5 that the only change observed in the spectrum when increasing the total number of dipoles from around 90 000 to nearly one-half of million lies in the slightly higher strength of the SPR. As a matter of fact, considering the poor gain that is actually achieved in this latter case, it is therefore concluded that our choice to use 2000 dipoles per sphere is sufficient to be fully confident in the quality of the reported spectra.

Furthermore, to ensure that the calculated absorption spectrum of the planar nanoparticle array was not sensitively dependent on the shape in which the nanoparticles were arranged, several arrangements differing by their shape were tested. In addition to the case of the hexagonally shaped array (Figure 1a), two other systems were designed by arranging the nanoparticles either in a square or in a circular shape, as illustrated in Figure 1b. The corresponding absorption spectra calculated for arrangements with the highest nanoparticle density, at various angles of incidence, are shown in Figure 6. The choice of comparing the different array shapes for the case of the highest nanoparticle concentration was preferred in order to make more obvious any effect that would potentially originate from the

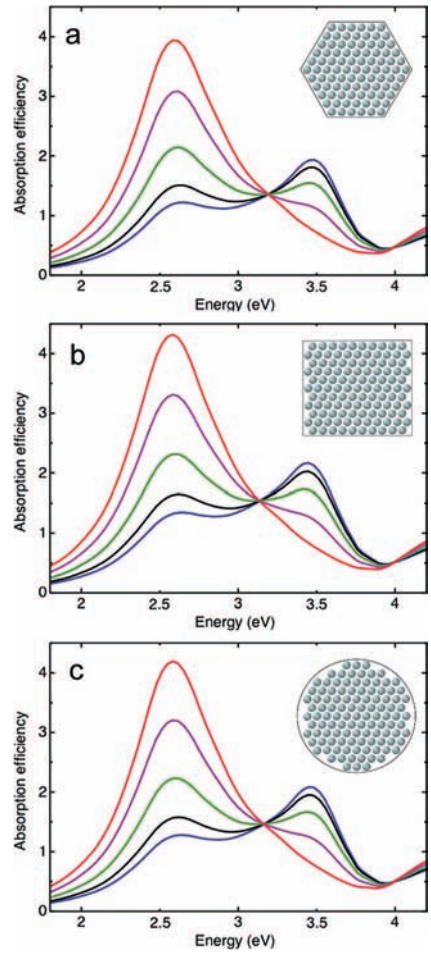

Figure 6. Calculated absorption spectra of N silver spheres forming a 2D hexagonal array arranged in (a) hexagonal, (b) square, and (c) circular shapes, with $N = 91$, 115, and 109 spheres, respectively. In each case, spectra corresponding to incidence angles of 0 (red), 30 (violet), 45 (green), 55 (black), and 60° (blue) are plotted. For all of these calculations, the relative interparticle spacing remains the same, that is, $d/(2R) = 0.25$, and an average number of around 2000 dipoles per sphere is used with the refractive index of the surrounding environment being $n_{ext} = 1.46$.

change in array shape. Without entering into a detailed description of each situation, it is reasonable to note that among hexagonal, square, and circular arrays, no dependence of the absorption spectra on the array shape is observable, whatever the incidence angle is. Such a statement is deduced from the basis of the three particular array shapes tested in this work but might be also available for most of the other shapes that could be designed in order to account for the 2D dimensionality of the planar array. This result argues in favor of the capability of the DDA method in properly modeling the optical response of an "infinite" planar close-packed arrangement of nanoparticles by designing a target in which only few particles need actually be involved.

IV. Conclusion

In this paper, we reported on DDA simulations of the optical absorption of 5 nm spherical silver nanoparticles hexagonally arranged in close-packed planar array. The profile of the calculated absorption spectra in the visible range is markedly dependent on the incidence of light on the system through the splitting of the dipolar surface plasmon band in two components when increasing the angle of incidence. This splitting clearly

reveals the optical anisotropy of the system formed by the planar arrangement of nanoparticles. In agreement with previous studies, the two absorption bands are assigned, in increasing order of energy, to the longitudinal and transverse plasmon modes, respectively. Besides, this band splitting has been observed to sensitively decrease for increasing interparticle spacing, as a result of the weakening of the dipolar interactions between particles in the system.

Therefore, it is expected that the optical response of 2D assemblies of silver nanoparticles can be tuned by controlling their interparticle spacing. Such a control should be achievable by synthesizing nanometer-sized metal nanoparticles via a chemical route and then by using different capping agents[47] to stabilize them or by growing a silica shell of controlled thickness on preformed metal nanoparticles.[48] These two approaches offer the possibility to vary the interparticle spacing in the 2D arrangement of nanoparticles. Further experimental studies are currently performed in order to compare photoabsorption measurements on real arrangements of nanoparticles to their optical response predicted by using the DDA method.

Acknowledgment. H.P. and M.-P.P. gratefully thank Pr. G. C. Schatz (Northwestern University) for fruitful discussions. The authors are also indebted to Pr. B. T. Draine (Princeton University) and Pr. P. J. Flatau (University of California) for making freely available the DDSCAT program. This work is partly supported by ANR in the frame of the PION research program (Project Number BLAN06-1_147266) and FAME network of excellence.

References and Notes

(1) Kreibig, U.; Vollmer, M. *Optical Properties of Metal Clusters*; Springer: New York, 1995.
(2) Charle, K. P.; Frank, F.; Schulze, W. *Ber. Bunsen-Ges. Phys.Chem. Chem. Phys.* **1984**, *88*, 350.
(3) Petit, C.; Lixon, P.; Pileni, M. P. *J. Phys. Chem.* **1993**, *97*, 12974.
(4) Jin, R. C.; Cao, Y. W.; Mirkin, C. A.; Kelly, K. L.; Schatz, G. C.; Zheng, J. G. *Science* **2001**, *294*, 1901.
(5) Pileni, M. P. *J. Phys. Chem. C* **2007**, *111*, 9019.
(6) Murphy, C. J.; San, T. K.; Gole, A. M.; Orendorff, C. J.; Gao, J. X.; Gou, L.; Hunyadi, S. E.; Li, T. *J. Phys. Chem. B* **2005**, *109*, 13857.
(7) Wiley, B. J.; Im, S. H.; Li, Z. Y.; McLellan, J.; Siekkinen, A.; Xia, Y. A. *J. Phys. Chem. B* **2006**, *110*, 15666.
(8) Link, S.; Wang, Z. L.; El-Sayed, M. A. *J. Phys. Chem. B* **1999**, *103*, 3529.
(9) Gaudry, M.; Cottancin, E.; Pellarin, M.; Lerme, J.; Arnaud, L.; Huntzinger, J. R.; Vialle, J. L.; Broyer, M.; Rousset, J. L.; Treilleux, M.; Melinon, P. *Phys. Rev. B* 2003, *67*.
(10) Kelly, K. L.; Coronado, E.; Zhao, L. L.; Schatz, G. C. *J. Phys. Chem. B* **2003**, *107*, 668.
(11) Sosa, I. O.; Noguez, C.; Barrera, R. G. *J. Phys. Chem. B* **2003**, *107*, 6269.
(12) Noguez, C. *J. Phys. Chem. C* **2007**, *111*, 3806.
(13) Bohren, C. F.; Huffman, D. R. *Absorption and Scattering of Light by Small Particles*; Wiley: New York, 1983.
(14) Lee, K. S.; El-Sayed, M. A. *J. Phys. Chem. B* **2005**, *109*, 20331.
(15) Schelm, S.; Smith, G. B. *J. Phys. Chem. B* **2005**, *109*, 1689.
(16) Jain, P. K.; Huang, X.; El-Sayed, I. H.; El-Sayad, M. A. *Plasmonics* **2007**, *2*, 107.
(17) Hutter, E.; Fendler, J. H. *Adv. Mater.* **2004**, *16*, 1685.
(18) Barnes, W. L.; Dereux, A.; Ebbesen, T. W. *Nature* **2003**, *424*, 824.
(19) Fendler, J. H.; Meldrum, F. C. *Adv. Mater.* **1995**, *7*, 607.
(20) Mie, G. *Ann. Phys.* **1908**, *25*, 377.
(21) Kerker, M. *The Scattering of Light and Other Electromagnetic Radiation*; Academic: New York, 1969.
(22) Zhao, J.; Pinchuk, A. O.; McMahon, J. M.; Li, S. Z.; Alisman, L. K.; Atkinson, A. L.; Schatz, G. C. *Acc. Chem. Res.* **2008**, *41*, 1710.
(23) Lerme, J. *Eur. Phys. J. D* **2000**, *10*, 265.
(24) Jensen, T.; Kelly, L.; Lazarides, A.; Schatz, G. C. *J. Cluster Sci.* **1999**, *10*, 295.
(25) Noguez, C. *Opt. Mater.* **2005**, *27*, 1204.
(26) Gonzalez, A. L.; Reyes-Esqueda, J. A.; Noguez, C. *J. Phys. Chem. C* **2008**, *112*, 7356.
(27) Zhao, L. L.; Kelly, K. L.; Schatz, G. C. *J. Phys. Chem. B* **2003**, *107*, 7343.
(28) Taleb, A.; Russier, V.; Courty, A.; Pileni, M. P. *Phys. Rev. B* **1999**, *59*, 13350.
(29) Russier, V.; Pileni, M. P. *Appl. Surf. Sci.* **2000**, *162*, 644.
(30) Pinna, N.; Maillard, M.; Courty, A.; Russier, V.; Pileni, M. P. *Phys. Rev. B* 2002, *66*.
(31) Taleb, A.; Petit, C.; Pileni, M. P. *Chem. Mater.* **1997**, *9*, 950.
(32) Purcell, E. M.; Pennypacker, C. R. *Astrophys. J.* **1973**, *186*, 705.
(33) Goodman, J. J.; Draine, B. T.; Flatau, P. J. *Opt. Lett.* **1991**, *16*, 1198.
(34) Draine, B. T.; Flatau, P. J. *J. Opt. Soc. Am.* **1994**, *11*, 1491.
(35) Draine, B. T. *Astrophys. J.* **1988**, *333*, 848.
(36) Draine, B. T.; Flatau, P. J. *Program DDSCAT 6.1*; University of California: San Diego, CA and Scripps Institution of Oceanography: La Jolla, CA.
(37) Draine, B. T.; Goodman, J. *Astrophys. J.* **1993**, *405*, 685.
(38) Jackson, J. D. *Classical Electrodynamics*; Wiley: New York, 1975.
(39) Hovel, H.; Fritz, S.; Hilger, A.; Kreibig, U.; Vollmer, M. *Phys. Rev. B* **1993**, *48*, 18178.
(40) Coronado, E. A.; Schatz, G. C. *J. Chem. Phys.* **2003**, *119*, 3926.
(41) Palik, E. D. *Handbook of Optical Constants of Solids*; Academic Press, Inc.: New York, 1985.
(42) Ashcroft, N. W.; Mermin, N. D. *Solid State Physics*; Holt-Saunders International Editions: Philadelphia, PA, 1976.
(43) Quinten, M.; Kreibig, U. *Appl. Opt.* **1993**, *32*, 6173.
(44) Haynes, C. L.; McFarland, A. D.; Zhao, L. L.; Van Duyne, R. P.; Schatz, G. C.; Gunnarsson, L.; Prikulis, J.; Kasemo, B.; Kall, M. *J. Phys. Chem. B* **2003**, *107*, 7337.
(45) Bouhelier, A.; Bachelot, R.; Im, J. S.; Wiederrecht, G. P.; Lerondel, G.; Kostcheev, S.; Royer, P. *J. Phys. Chem. B* **2005**, *109*, 3195.
(46) Ghosh, S. K.; Pal, T. *Chem. Rev.* **2007**, *107*, 4797.
(47) Motte, L.; Pileni, M. P. *Appl. Surf. Sci.* **2000**, *164*, 60.
(48) Pastoriza-Santos, I.; Perez-Juste, J.; Liz-Marzan, L. M. *Chem. Mater.* **2006**, *18*, 2465.

JP810478R